


A. ZHAO 
L. ZHANG
Y. PANG
C. YE

Ordered tellurium nanowire arrays and their optical properties

Laboratory of Functional Nanomaterials and Nanostructures, Institute of Solid State Physics, Chinese Academy of Sciences, Hefei 230031, P.R. China

Received: 11 July 2003/Accepted: 30 October 2003
Published online: 28 January 2004 • © Springer-Verlag 2004

ABSTRACT High-density tellurium (Te) nanowire arrays were prepared in the nanochannels of an anodic aluminum membrane (AAM) template using the electrochemical deposition method. The as-synthesized Te nanowires, typically 60 nm in diameter and up to 40 μm in length, possess a hexagonal single crystalline structure following [001] growth direction. The optical polarization properties of Te nanowire arrays embedded in AAM were investigated using an optic parameter oscillator in the wavelength range from 0.7 to 1 μm . The high optical polarization of the Te nanowire arrays embedded in the AAM assembly system was observed.

PACS 81.05.Cy; 78.67.-n; 82.80.Fk.

1 Introduction

With the development of various photonic nanodevices, there has been increasing interest in optical studies of one-dimensional nanostructures because of their numerous potential applications in photonic nanodevices [1–4]. Among them, a high quality of linearly polarized light produced by a nanometer-sized polarizer may prove useful to integrated photonic circuits, optical switches and interconnects, near-field imaging, and high-resolution detectors [2–4]. The light polarization properties of semiconductor nanowires are interesting due to their high polarization, such as InP [4] and CdSe [5]. Furthermore, the polarization property of nanostructure semiconductors can be tailored by suitably adjusting their size. On the other hand, the light polarization properties of well-aligned metal nanowire arrays have been studied in theory and experiments [6, 7]. Recently we have also investigated metal nanowires arrays for polarizers [8, 9]. However, the light polarization properties of the semiconductor nanowire arrays have not been studied. Tellurium is a narrow bandgap semiconductor. Hexagonal Te has a highly anisotropic crystal structure consisting of helical chains of covalent bound atoms, which are in turn bound together through van der Waals interactions into a hexagonal lattice, and the C

axis is perpendicular to the plane consisting of six Te atoms. This special crystal structure leads to the inherent anisotropy of hexagonal Te [10, 11]. Previously, Te nanowire arrays were prepared by injecting melted Te in a reactor of a high temperature–high pressure injection apparatus [12]. But the crystalline structure of Te was not mentioned in this paper. Recently, several research groups have successfully prepared Te nanotubes, nanorods, and nanobelts using the solution phase approach and hydrothermal route, respectively [13, 14]. Here, we report synthesis of high ordered Te nanowire arrays embedded in AAM by a simply electrochemical deposition approach at room temperature. The light polarization properties of Te nanowire arrays embedded in AAM were investigated.

2 Experimental

2.1 Synthesis of Te nanowire arrays

The anodic alumina membranes used in our experiments were prepared by a two-step anodization process as described previously [15]. Briefly, the AAM was formed by anodizing an aluminum foil in 0.3 M oxalic acid solution under constant voltage 40 V. A remaining aluminum layer existing at the bottom of the alumina membrane was removed in 1 M CuCl_2 solution. Subsequently, the pore bottom was opened by chemical etching in 5 wt. % phosphoric acid solution, and the nanochannel diameter (40–90 nm) was adjusted by immersing it in the solution for different times. A layer of Au was deposited onto one side of the templates by vacuum evaporation to serve as the working electrode. The electrochemical deposition of Te nanowire arrays was carried out in a three-electrode electrochemical cell at room temperature. The counter electrode was a pure graphite plate and the AAM template with Au layer was used as the working electrode, and with a saturated calomel electrode (SCE) serving as the reference electrode. The electrolyte was an aqueous solution of HTeO_2^+ at about 4×10^{-4} M that was added in the form of TeO_2 (the solubility of TeO_2 depends on the pH [16]). The pH value of the solution was adjusted to about 2.0 by adding hydrochloric acid. The electrochemical deposition process was carried out for 24 hours at room temperature with a deposition potential of -400 mV vs. SCE. After deposition, the obtained samples were rinsed several times with ethanol and de-ionized water, and then dried in air at room temperature.

2.2 Sample characterization

Powder X-ray diffraction (XRD, Philips PW 1700x with $\text{Cu K}\alpha$ radiation), transmission electron microscopy (TEM, Philips CM200, operated at 200 kV), field-emission scanning electron microscopy (FE-SEM, JEOL JSM-6700F) and high-resolution transmission electron microscopy (HREM, JEOL 2010, operated at 200 kV) were used to study crystalline structures and morphologies of nanowire arrays. The chemical composition of the nanowires was determined by X-ray energy dispersive spectroscopy (EDS) attached to the HREM. For TEM and HREM characterization, the as-deposited samples were treated with 5 wt. % NaOH solution for 5 min at room temperature to dissolve the AAM template, followed by dispersing the Te nanowires in ethanol by ultrasonication. A drop of the suspension was deposited onto carbon film coated holey copper grids to be mounted on the TEM and HREM specimen holder.

2.3 Optical loss measurement of sample

The optical loss of the samples was evaluated by the measurement system of an optic parameter oscillator. For optical measurement, a portion of as-deposition sample was sliced off, and the cross-sectional surface was polished until $\sim 10 \mu\text{m}$ thickness. The sample was stuck on to a SiO_2 glass slide for mechanical support in the optical measurement. Subsequently, the sample was positioned on a rotating stage so that the direction of polarization could be adjusted to either parallel or perpendicular to the nanowire axis.

3 Results and discussion

3.1 Structure and morphology of Te nanowire arrays

Figure 1a shows the typical FE-SEM images, from which it can be clearly seen that Te nanowires were filled well in nanochannels of the AAM. Figure 1b exhibits a TEM image of an individual Te nanowire detached from AAM. The selected area electron diffraction pattern on this single wire (inset) can be indexed as a nanowire with a hexagonal phase of a single crystalline Te, which is in agreement with the XRD results. The XRD spectra taken from the sample

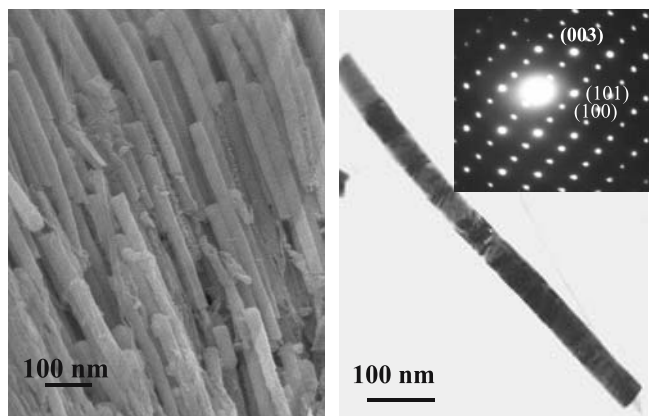


FIGURE 1 a FE-SEM image of Te nanowire arrays embedded in AAM. b The TEM image of an individual Te nanowire with a diameter of about 60 nm detached from AAM

is shown in Fig. 2. All the diffraction peaks could be indexed to a hexagonal phase of Te (JCPDS 36-1452). Among all peaks, the (003) peak is relatively intensive, which implies that the Te nanowires grew along a preferential direction [001]. The crystal structures were further examined by a high-resolution transmission electron microscopy. The HREM image in Fig. 3 reveals clearly that the Te nanowire is single crystalline. It can also be seen that the nanowire surface in atomic scale is still smooth. The lattice-resolved image shows that the Te nanowires are defect-free single crystals, and the (100) and (003) atomic planes with lattice spacing around 0.385 nm and 0.199 nm, respectively, are clearly revealed. The (003) planes are perpendicular to the long axis of the Te nanowire, indicating that the Te

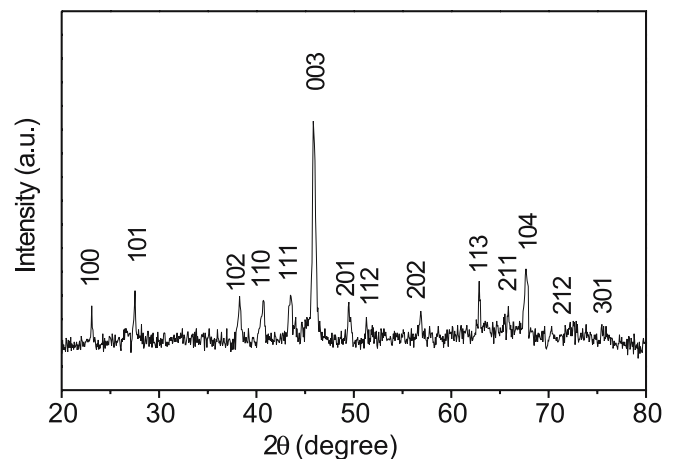


FIGURE 2 XRD patterns taken from Te nanowire arrays/AAM

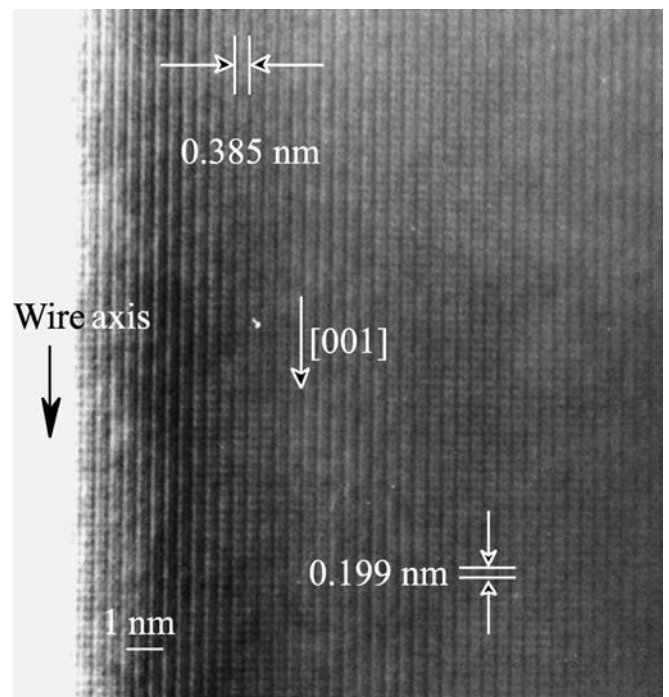
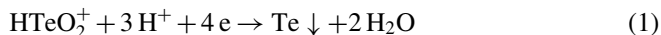


FIGURE 3 The lattice-resolved image of the Te nanowire displays the (100) and (003) lattice planes with lattice spacing around 0.385 nm and 0.199 nm, respectively. The (003) planes are vertical to the long axis of the Te nanowire

nanowire has the preferential growth direction of [001] (i.e. C axis) along the nanowire axis, in agreement with the XRD results. The growth of Te nanowires in the nanochannels evolves the process of charged ions running into the nanochannels of AAM and subsequently reacting at the cathode. The reaction on the cathode can be expressed by the following [17]:



3.2 The polarization properties of Te nanowire arrays

Optical polarization of the Te nanowire arrays embedded in AAM was investigated by illuminating them with a polarized light in the wavelength range from 0.7 to 1 μm . The direction of polarization is designated as parallel or perpendicular polarization depending upon whether the electric field of light is parallel or perpendicular to the nanowire axis (i.e. C axis). Figure 4 shows the optical loss of the sample, which was calculated from the ratio of the intensity of transmitted beam with and without the sample. Curves $L_{//}$ and curves L_{\perp} denote the optical loss of the sample by illuminating them with parallel and perpendicular incident light, respectively. While the optical loss for perpendicular polarization is around 0.7 dB, the optical loss for parallel polarization is as large as around 12 dB. It indicated the prominent light polarization properties of the sample. However, it cannot be proved that the polarization of sample is linearly polarized. So we further measured the intensity of transmission light when the polarized direction of incident light rotated from parallel to perpendicular (shown in Fig. 5). The data could be fitted to Malus's law [18] ($I = I_0 \cos^2 \theta$, θ is the polarization angle, I and I_0 are intensity and maximum intensity of transmitted light, respectively). The good agreement of the theoretical and experimental data suggests that transmitted light through the Te nanowire arrays embedded in AAM is nicely linearly polarized. The polarization ratios are calculated as 0.85 according to $\rho = (I_{\max} - I_{\min}) / (I_{\max} + I_{\min})$, I_{\max} and I_{\min} present the maximum and minimum intensities, i.e. parallel and perpendicular to the wire axis, respectively.

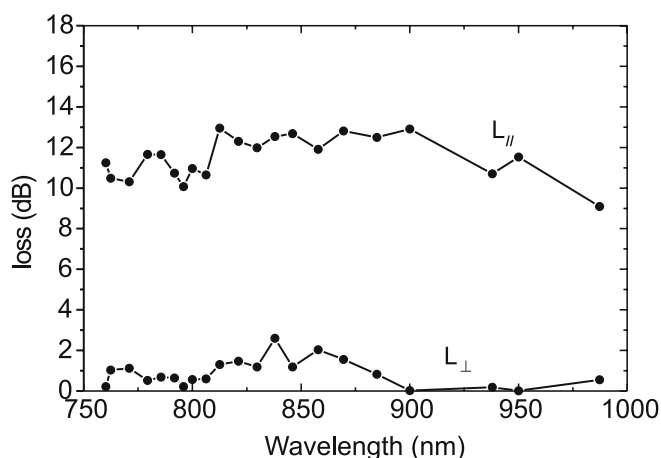


FIGURE 4 Optical loss of Te nanowire arrays embedded in an AAM sample measured in the range from 0.75 to 1 μm wavelength

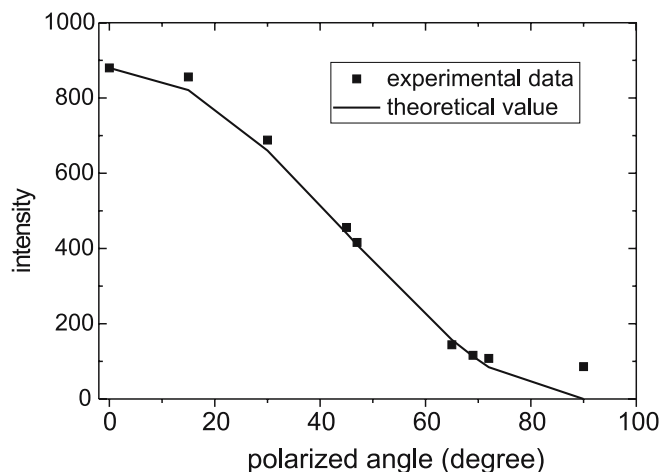


FIGURE 5 Variation of transmission intensity as a function of the incident polarization angle with respect to the nanowire axis. Curve: theoretical fitting, square: experimental data

The high light polarization of Te nanowire arrays embedded in AAM could be attributed to two aspects. The first aspect comes from the natural anisotropy of hexagonal Te. Previous studies have shown that bulk Te has high anisotropy on resistivity between parallel and perpendicular to C axis [19]. The second aspect includes a cylindrical, strongly confining potential for both electrons and holes in high anisotropy of a one dimension nanostructure [3, 4, 18]. The wavelength of incidence is much greater than the diameter of nanowires. When the electric vectors of incident are parallel to the wire axis, they can drive the charge carriers moving along the wires. In this process, there are the light absorption and reflection due to collision with the lattice and reradiating in a backwards direction, respectively [18]. So the intensity of transmitted light was attenuated. While the electric vectors of incident are perpendicular to the wire axis, the charge carriers cannot move across the narrow lateral orientation. So the incident cannot be reduced to when they transmitted the sample. Consequently, we can see the result that the transmittance of the parallel incidence is much higher than that of the perpendicular incidence.

4 Conclusion

In summary, ordered Te nanowire arrays were grown by the electrochemical method in AAM. The high optical linear polarization of the Te nanowire arrays embedded in AAM was observed, which accounted for the cooperation of the natural anisotropy of hexagonal Te and anisotropy of one dimension confinement. It could be useful in integrated photonic circuits, optical switches and interconnects, near-field imaging, and high-resolution detectors.

ACKNOWLEDGEMENTS This work was supported by the National Major Project of Fundamental Research: Nanomaterials and Nanostructures (Grant No. 19994506), and Natural Science Foundation of China (Grant No. 19974055).

REFERENCES

- 1 T. Someya, H. Akiyama, H. Sakaki: Phys. Rev. Lett. **74**, 3664 (1995)
- 2 X. Duan, Y. Huang, Y. Cui, J. Wang, C.M. Lieber: Nature **409**, 66 (2001)

- 3 F. Vouilloz, D.Y. Oberli, M.-A. Dupertuis, A. Gustafsson, F. Reinhardt, E. Kapon: *Phys. Rev. B* **57**, 12 378 (1998)
- 4 J. Wang, M.S. Gudiksen, X. Duan, Y. Cui, and C.M. Lieber: *Science* **293**, 1455 (2001)
- 5 J. Hu, L.s. Li, W. Yang, Liberato Manna, Lin-wang Wang, A. Paul Alivisatos: *Science* **292**, 2060 (2001)
- 6 M. Saito, M. Miyagi: *Appl. Opt.* **28**, 3529 (1989)
- 7 M. Saito, M. Kiriwara, T. Taniguchi, M. Miyagi: *Appl. Phys. Lett.* **55**, 607 (1989)
- 8 Y.T. Pang, G.W. Meng, L.D. Zhang, Y. Qin, X.Y. Gao, A.W. Zhao: *Adv. Mater.* **12**, 719 (2002)
- 9 Y.T. Pang, G.W. Meng, Y. Zhang, Q. Fang, L.D. Zhang: *Appl. Phys. A* **76**, 533 (2003)
- 10 T. Ikari, H. Berger, F. Levy: *Mater. Res. Bull.* **21**, 99 (1986)
- 11 K. Araki, T. Tanaka: *Jpn. J. Appl. Phys.* **11**, 472 (1972)
- 12 C.A. Huber, T.E. Huber, M. Sadoqi, J.A. Lubin, S. Manalis, C.B. Prater: *Science* **263**, 800 (1994)
- 13 B. Mayers, Y. Xia: *J. Mater. Chem.* **12**, 1875 (2002)
- 14 M. Mo, J. Zeng, X. Liu, W. Yu, S. Zhang, Y. Qian: *Adv. Mater.* **14**, 1658 (2002)
- 15 Y. Du, W.L. Cai, C.M. Mo, J. Chen, L.D. Zhang, X.G. Zhu: *Appl. Phys. Lett.* **74**, 2951 (1999)
- 16 C. Lepiller, P. Cowache, J.F. Guillemoes, N. Gibson, E. Özsan, D. Lincot: *Thin Solid Films* **361–362** 118 (2000)
- 17 E. Morri, C.K. Backer, J.K. Keynolds, K.W. Raicsh: *Electroanal. Chem.* **252**, 441 (1988)
- 18 W.H.A. Fincham, M.H. Freeman: *Optics*, 9th (Butterworth Inc., Boston 1980)
- 19 R.A. Smith: *Semiconductors* (Cambridge University press: Cambridge 1961)